Characterization of the β-Carbon Processing Reactions of the Mammalian Cytosolic Fatty Acid Synthase: Role of the Central Core†

Andrzej Witkowski, Anil K. Joshi, and Stuart Smith*

Children's Hospital Oakland Research Institute, 5700 Martin Luther King, Jr., Way, Oakland, California 94609

Received May 18, 2004; Revised Manuscript Received June 15, 2004

ABSTRACT: The properties of the β-ketoacyl reductase, dehydrase, and enoyl reductase components of the animal fatty acid synthase responsible for the reduction of the β-ketoacyl moiety formed at each round of chain elongation have been studied by engineering and characterizing mutants defective in each of these three catalytic domains. These "β-carbon processing" mutants leak the stalled four-carbon intermediates by direct transfer to CoA. However, enoyl reductase mutants leak β-ketobutyryl, β-hydroxybutyryl, and crotonyl moieties, a finding explained, at least in part, by the observation that the equilibrium and rate constant for the dehydrase reaction favor the formation of β-hydroxy rather than enoyl moieties. In this regard, the type I animal fatty acid synthase resembles its type II counterpart in *Escherichia coli* in that both systems rely on the enoyl reductase to pull the β-carbon processing reactions to completion. Kinetic and nucleotide binding measurements on fatty acid synthases mutated in either of the two nucleotide binding domains revealed that the NADPH binding sites are nonidentical, the enoyl reductase exhibiting higher affinity. Surprisingly, NADPH binding is also completely compromised by certain deletions and mutations in the central core region distant from the nucleotide binding sites. Comparable central core sequences are present in the structurally related modular polyketide synthases, except in those modules that lack all three β-carbon processing enzymes. These findings suggest that the central core region of fatty acid and polyketide synthases plays an important role in facilitating the β-carbon processing reactions.

The synthesis of fatty acids de novo in animals is catalyzed by a cytosolic, homodimeric protein, the fatty acid synthase (FAS),[1] that contains seven discrete functional domains on both of the 272 kDa subunits (*1*, *2*). These domains cooperate to achieve the sequential extension of an alkanoic chain, two carbon atoms at a time, by a series of decarboxylative condensation reactions, each of which is followed by the reduction of the β-ketoacyl condensation product to a saturated acyl moiety. The elongation process is normally terminated by intervention of the thioesterase domain of the FAS when the chain length of the saturated acyl moiety reaches 16 carbon atoms. Reduction of the β-ketoacyl condensation product involves the sequential action of three different enzymes, the β-ketoacyl reductase, dehydrase, and enoyl reductase, that collectively are referred to as the β-carbon processing enzymes. The stereochemistry of these reactions was elucidated several years ago and involves the reduction of the 3-ketoacyl moiety to a (3*R*)-hydroxyacyl moiety with transfer of the prochiral 4*S* hydrogen of NADPH, dehydration to a *trans*-enoyl moiety by the syn elimination of the prochiral 2*S* hydrogen and the 3*R* hydroxyl as water, and finally reduction to a saturated acyl moiety by transfer of the prochiral 4*R* hydrogen of NADPH to the prochiral 3*R* hydrogen and transfer of solvent hydrogen to the prochiral 2*S* position (*3*). However, characterization of the nucleotide binding sites has been hampered by difficulties in distinguishing between the two sites, and only recently has it become possible to apply mutagenesis to circumvent this problem. The active site of the dehydrase domain was originally identified from the presence of a HxxxGxxxxP motif found characteristically in dehydrases and has been confirmed by mutagenesis (*4*) (Figure 1). The NADPH binding sites were initially identified by recognition of the characteristic glycine-rich motif GxGxxG/AxxxA in a region predicted to form a tight turn between the first β-sheet and α helix of a "Rossmann fold", together with a basic region further downstream (*6*, *7*) (Figure 1). The first glycine residue in the motif is believed to be necessary to permit access of the pyridine nucleotide, since the presence of side chains in the turn would block access of the cofactor (*8*). The downstream basic residues typically are found in NADPH-specific binding sites, where they provide a nest of positive charge for interaction with the 2-phosphate of NADPH (*9*). The objectives of this study were to authenticate separately the β-ketoacyl reductase and enoyl reductase nucleotide binding sites by mutagenesis, to assess the overall kinetic properties of the three β-carbon processing enzymes, and to evaluate the effects on product formation of blocking each of these reactions. Finally, the possibility that sequence elements outside of the three catalytic domains might be important for maintaining the integrity of the β-carbon processing functions was investigated by deletion and replacement mutagenesis within the central core region of the FAS.

† This work was supported by Grant DK 16073 from the National Institutes of Health.

* To whom correspondence should be addressed. Phone: (510) 450-7675. Fax: (510) 450-7910. E-mail: ssmith@chori.org.

[1] Abbreviations: FAS, fatty acid synthase; ACP, acyl carrier protein; PKS, polyketide synthase.

10.1021/bi048988n CCC: $27.50
Published on Web 07/22/2004

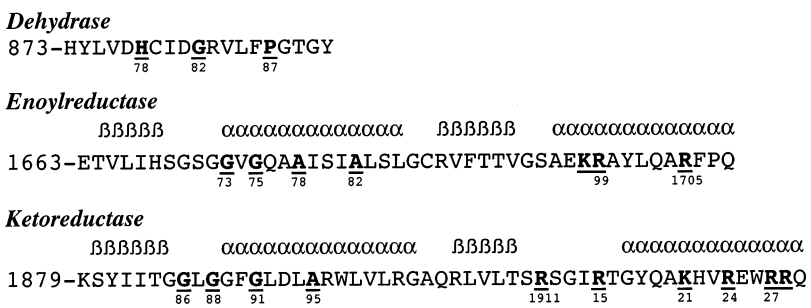

FIGURE 1: Location of the active site region of the dehydrase and nucleotide binding regions of the enoyl and β-ketoacyl reductase domains of the animal FAS. The locations of residues believed to represent characteristic sequence motifs are indicated in boldface, underlined characters. Secondary structures for the two reductases, shown above the sequences, were predicted using Predictprotein (*5*).

EXPERIMENTAL PROCEDURES

Construction of cDNAs Encoding His_6- and FLAG-Tagged FASs and Expression of the Proteins in Sf9 Cells. The strategy for construction of cDNAs encoding the wild-type FAS, domain-specific mutants and incorporation of a His_6 or FLAG tag has been described in detail elsewhere (*4*, *10*−*13*). In vitro site-directed mutagenesis was carried out by the overlap PCR method (*14*), using Vent DNA polymerase. Details of the strategies employed to generate DH^- (His878Ala) and various ER^- and KR^- mutants were described previously (*4*, *7*). The final FAS cDNA constructs, in the context of the pFASTBAC1 vector (FB), were used to generate recombinant baculoviral stocks by the transposition method employing the BAC-to-BAC baculovirus expression system, according to the manufacturer's instructions. *Sf*9 cells were infected with the purified recombinant viruses and cultured for 48 h at 27 °C. The tagged FAS proteins were purified from the cytosols as described earlier (*15*). Details of the procedures for engineering core deletion and replacement mutants and the sequences and location of the primers used are available as Supporting Information. These proteins, which were all C-terminally His_6-tagged, were purified by a single-step, metal ion affinity chromatography procedure.

Separation of the Dimeric and Higher Oligomeric Forms of the R1508A FAS Mutant. The R1508A FAS mutant purified by nickel affinity chromatography (single band on SDS−PAGE) contained a mixture of dimers and higher oligomers, as revealed by gel filtration (BioSep-Sec-S3000, 300 × 7 mm; Phenomenex) in 0.2 M potassium phosphate, pH 7, and 1 mM EDTA. The dimers and higher oligomers were separated first by anion-exchange chromatography on a 1 mL column of HiTrap Q HP (Amersham Biosciences) using a gradient of 50−250 mM potassium phosphate, pH 7, over 30 min; buffers contained 1 mM EDTA, 1 mM DTT, and 10% glycerol. Dimers and higher oligomers were eluted with 100 and 165 mM phosphate, respectively. The higher oligomers were purified further by gel filtration.

Reductase Assays. β-Ketoacyl reductase activity was monitored spectrophotometrically at 340 nm using either *trans*-1-decalone (*10*) or β-ketobutyryl-CoA (*12*) as substrate. Enoyl reductase activity was monitored spectrophotometrically at 340 nm using crotonyl-CoA as substrate (*12*). In some experiments where very high concentrations of NADPH or NADH were used, the absorbance was recorded at 400 nm.

Dehydrase Assay. Activity of the dehydrase domain of the FAS was assessed in the forward direction using the *S*-β-hydroxybutyryl thioesters of either *N*-acetylcysteamine or CoA and in the backward direction using the crotonyl thioesters of either *N*-acetylcysteamine or CoA. Assay mixtures containing 0.1 M potassium phosphate buffer (pH 7), substrate, and enzyme were incubated at 37 °C, and the progress of the reaction was monitored spectrophotometrically at 270 nm. For estimation of the reaction equilibrium, CoA esters were used as substrates, and the reaction mixtures also contained free CoA (50 μM); the reactions were stopped by the addition of perchloric acid (10% final concentration), protein was removed by centrifugation, the supernatant was adjusted to pH 5.5, and the proportion of *S*-β-hydroxybutyryl-CoA and crotonyl-CoA present was determined by HPLC, as described in the section Product Analysis.

Kinetics. Kinetic parameters were determined from six independent plots of the experimental data, 7−20 points per plot (Lineweaver−Burk, Eadie−Hofstee, Hanes−Woolf, Johansen−Lumry, direct linear plot, and nonlinear regression), using the program Enzyme Kinetics (Trinity Software). Results are reported as means ± standard deviations.

Measurement of NADPH Binding by Fluorescence Enhancement. Fluorescence was measured with a Perkin-Elmer Life Sciences LS50B luminescence spectrometer equipped with a thermojacketed cuvette holder, maintained at 22 °C, and a rectangular quartz cell (1 × 1 cm). Excitation was set at 340 nm, and emission was monitored mostly between 440 and 470 nm using a slit width of 3 and 6 nm for excitation and emission, respectively. When fluorescence emittence, β′, of bound ligand was estimated, emission spectra were scanned between 400 and 480 nm. FAS was prepared at 1 mg/mL in 0.25 M potassium phosphate, pH 7, containing 1 mM EDTA, 1 mM dithiothreitol, and 10% glycerol and filtered through a 0.25 μm low-protein binding filter, and the UV spectrum was recorded. Titration with NADPH, freshly prepared in the same buffer, was done by successive additions of 2.5 μL portions to a cuvette containing either FAS solution or buffer alone (0−18 μM NADPH in the assay). Appropriate corrections were made for volume changes. Fluorescence intensity was corrected for the absorbance of exciting light according to the formula $F_{av}/F_0 = 10^{-0.5A}$, where F_{av} and F_0 are average and original fluorescence intensity, respectively, of exciting light and A is NADPH absorbance at 340 nm. NAPDH absorbance was calculated from the corrected NADPH concentration using the molar extinction coefficient 6220 M^{-1} cm^{-1}. Corrected fluorescence emission of NADPH was linear throughout the concentration range tested. Fluorescence enhancement was determined from the difference of NADPH fluorescence

intensities in the presence and absence of FAS. The dissociation constants and number of binding sites were calculated from eqs 1−3 according to Pry and Hsu (*16*), where β and β' are fluorescence emittence of free and enzyme-bound NADPH, respectively.

$$F = \beta[\text{NADPH}]_f + \beta'[\text{NADPH}-\text{FAS}] \quad (1)$$

$$K_D = [\text{FAS}]_f[\text{NADPH}]_f/[\text{NADPH}-\text{FAS}] \quad (2)$$

$$[\text{NADPH}]_t = [\text{NADPH}]_f + [\text{NADPH}-\text{FAS}] \quad (3)$$

The β value determined from the $F = f([\text{NADPH}])$ plot was 33.8−34.0. The β' was first calculated from eq 1 assuming that at high FAS and low NADPH concentrations, >8 μM (subunit) and 65 nM, respectively, all NADPH was bound and $[\text{NADPH}]_f$ was zero. The dissociation constant and number of binding sites were then calculated from the Scatchard plot, based on the assumption of a single class of equivalent and noninteracting binding sites. The concentration of bound NAPDH was obtained from eq 4 that was derived by substitution of eq 3 into eq 1.

$$[\text{NADPH}-\text{FAS}] = (F - \beta[\text{NADPH}]_t)/(\beta' - \beta) \quad (4)$$

The calculated dissociation constant was then used to reevaluate the concentration of free NADPH in the β' estimation, and a new β' value was assessed on the basis of eq 1 and used in the Scatchard plot again. The calculations were iterated until further processing produced only minimal changes in the dissociation constant and binding site values. Usually one to five iterations were sufficient to finalize calculations.

Product Analysis. Assay mixtures, in a final volume of 100 μL, containing 0.2 M potassium phosphate (pH 6.6), 0.19 mM NADPH, 40 μM AcCoA, 1.5 or 15 μg of FAS, and, if added, 100 μM CoASH were preincubated at 37 °C for 1 min. Reactions were started by addition of [2-^{14}C]-malonyl-CoA (100 μM final concentration), and incubation was continued for 2 min. Reactions were stopped by addition of perchloric acid to a final concentration of 10% or 6%, when either the acyl-CoA pool or free fatty acids was analyzed, respectively.

Samples for acyl-CoA analysis were centrifuged; the supernatant was diluted with starting buffer and chromatographed on a column of C18 SpheriSorb, 300 Å, 5 μm, 4.6 × 250 mm (PhaseSeparation Ltd., Deeside, Clwyd, U.K.), in 50 mM sodium phosphate buffer (pH 5.5) for 5 min followed by a five-step gradient, to 27% 50 mM sodium phosphate (pH 5.5)/10% acetonitrile over 5 min, to 37% 50 mM sodium phosphate (pH 5.5)/10% acetonitrile over 10 min, to 53.5% 50 mM sodium phosphate (pH 5.5)/10% acetonitrile over 10 min, to 100% 50 mM sodium phosphate (pH 5.5)/10% acetonitrile over 10 min, and to 100% 50 mM sodium phosphate (pH 5.5)/40% acetonitrile over 10 min. The flow rate was maintained at 1 mL/min. Components in the effluent were detected by liquid scintillation spectrometry and/or from absorbance at 260 nm.

Free fatty acids were extracted with hexane/2-propanol (3:2), derivatized with Phenacyl-8 (*17*), and separated on a Phenyl Intersil 5 μm, 4.6 × 150 mm, column (MetaChem Technologies, Torrance, CA). The column was developed at 1.5 mL/min in water/62% acetonitrile for 5 min; then the acetonitrile concentration was increased over 20 min to 95% and the elution continued for 10 min.

Table 1: Kinetic Parameters for β-Ketoreductase Mutants

	trans-decalone reductase activity		
β-ketoacyl reductase mutant	k_{cat} (s^{-1})	K_m(NADPH) (μM)	k_{cat}/K_m ($s^{-1}\,\mu M^{-1}$)
wild type[a]	73.0 ± 1.9	20 ± 2	3.65
G1888A	7.3 ± 1.2	902 ± 251	0.0081
G1886F	1.1 ± 0.1	2700 ± 610	0.0004

[a] The G1675T, G1672V mutant defective in enoyl reductase activity was used.

Dynamic Light Scattering. Dynamic light scattering properties of different FAS mutants, 0.4−0.5 mg/mL, were measured with DynaPro-MS/X with Dynamics v.6 software (Protein Solutions) in a 12 μL optical cell at 25 °C according to manufacturer's recommendations.

Dynamic light scattering analyses gave hydrodynamic radii of 10.17 ±0.05, 10.40 ±0.20, and 9.85 ±0.15 nm for wild-type FAS, the R1508A dimer, and the double V/A, K/G FAS mutant, respectively. Assuming ideal spherical protein shape and a partial specific volume of 0.73 mL/g, molecular masses of 759 ±7, 809 ±39, and 710 ± 25 kDa, respectively, were calculated. The actual mass of the FAS dimer is 544 kDa, and the higher than expected values likely result from the inherent asymmetry of the FAS dimer (*18*, *19*).

RESULTS

Catalytic Activities of FASs Carrying Mutations in the Putative Nucleotide Binding Regions of the Two Reductase Domains. Introduction of side chains at positions 1670 (G1670A, G1670S) or 1675 (G1675A) within the glycine-rich region of the putative nucleotide binding region of the enoyl reductase had no effect on either enoyl reductase or overall FAS activity. However, replacement of the glycine residues at positions 1672 (G1672V) or 1673 (G1673Y) almost completely eliminated both activities. Similarly, replacement of the glycine residues at either position 1886 or position 1888 within the putative β-ketoacyl reductase nucleotide binding site dramatically lowered both β-ketoacyl reductase and FAS activity. Neither the G1672V nor G1673Y mutants retained sufficient activity to permit evaluation of the effect on the kinetics of NADPH binding at the enoyl reductase domain. However, the high turnover number of the β-ketoacyl reductase exhibited with *trans*-1-decalone as substrate allowed determination of the NADPH kinetic parameters of the two β-ketoacyl reductase mutants. The K_m values for both of the G1888A and G1886A mutants were increased about 2 orders of magnitude, and catalytic efficiency was reduced 3−4 orders of magnitude, compared to the FAS carrying a wild-type β-ketoacyl reductase domain (Table 1).

The availability of mutant FASs defective in only one of the two nucleotide binding domains provided an opportunity to study the kinetics and pyridine nucleotide binding at each site without the possibility of interaction with, or interference from, the second site. Kinetic parameters for both NADPH and NADH were derived for the β-ketoacyl and enoyl reductase using β-ketobutyryl-CoA and crotonyl-CoA, respectively, as substrates (Table 2). In addition, the β-ketoacyl reductase activity was assessed using the model substrate

Table 2: Kinetic Parameters for the β-Ketoacyl and Enoyl Reductases Using NADPH and NADH

	β-ketoacyl reductase[a]				enoyl reductase[b]	
	trans-decalone reductase		β-ketobutyryl-CoA reductase		crotonyl-CoA reductase	
parameter	NADPH	NADH	NADPH	NADH	NADPH	NADH
k_{cat} (s^{-1})	73 ± 2	1.1 ± 0.09	0.8 ± 0.0	1.1 ± 0.13	9.8 ± 0.5	0.12 ± 0.01
K_m (μM)	20 ± 2	500 ± 47	8.7 ± 0.4	820 ± 220	6.5 ± 0.6	121 ± 24
k_{cat}/K_m ($s^{-1}\mu M^{-1}$)	3.7	0.0022	0.092	0.0013	1.5	0.0010

[a] The G1675T,G1672V mutant defective in enoyl reductase activity was used. [b] The G1888A mutant defective in β-ketoacyl reductase activity was used. Both FAS mutants were C-terminally FLAG-tagged.

trans-1-decalone, which is reduced directly without formation of a covalent acyl-enzyme intermediate. NADPH exhibited high affinity for both reductase sites (K_m values in the low micromolar range) and was about 3 orders of magnitude more efficient (k_{cat}/K_m) than NADH as the hydrogen donor for both reductases. The k_{cat} values for the β-ketoacyl reductase obtained with NADPH are considerably higher when *trans*-decalone, rather than β-ketobutyryl-CoA, is used as substrate, suggesting that transfer of the β-ketobutyryl substrate onto the ACP and transfer of the product (β-hydroxybutyryl and/or crotonyl moieties) back to CoA may be rate limiting.

Binding of NADPH to the β-Ketoacyl Reductase and Enoyl Reductase Domains. The availability of FASs defective in either of the two nucleotide binding domains afforded the possibility of studying the binding of pyridine nucleotides to each of the two sites individually. Two FAS mutants, G1673Y and G1888A, both C-terminally His-tagged, were employed in measurements of NADPH binding to the β-ketoacyl and enoyl reductase domains, respectively. The G1673Y and G1888A mutations introduced into Rossmann motifs within the enoyl reductase and β-ketoacyl reductase domains, respectively, resulted in specific inhibition of the targeted activities and loss of FAS activity (*7*). The fluorescence enhancement assays demonstrated the existence of two different pairs of NADPH binding sites in the FAS dimer (Figure 2). Compared with the NADPH binding site in the β-ketoacyl reductase domain, that in the enoyl reductase domain exhibited 3.7-fold higher affinity for NADPH and displayed only ~25% of the fluorescence enhancement upon NADPH binding. The combined fluorescence enhancement data for the β-ketoacyl and enoyl reductase mutants (Figure 2, dashed line) were in very good agreement with those obtained for the wild-type FAS, indicating that the NADPH binding sites function independently.

Effect of Mutations in the β-Carbon Processing Enzymes on Product Formation. In a typical reaction with the wild-type FAS, more than 97% of the malonyl-CoA utilized is converted to long-chain fatty acid (Table 3). However, small amounts of all of the 4-carbon intermediates leak off the enzyme, by transfer to CoA, and a trace amount of triacetic lactone is formed as the result of the unreduced β-ketobutyryl intermediate undergoing a second condensation reaction. The CoA required for release of the 4-carbon products is generated as a result of the transfer of the acetyl and malonyl substrate moieties from the CoA thioester to the FAS. When this CoA pool is elevated by direct addition to the reaction mixture, the amount of 4-carbon products leaking from the FAS is increased, although overall malonyl-CoA utilization is inhibited (Table 3). Regardless of CoA availability, the major 4-carbon esters formed are β-ketobutyryl- and butyryl-CoA.

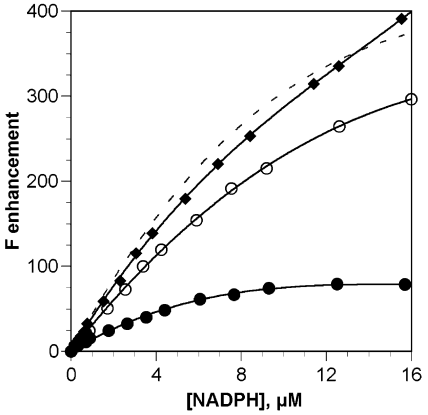

	ß'	Kd	n
	μM-1	*μM*	*mole/dimer*
G1888A FAS	71	4.2	1.6
G1673Y FAS	189	15.6	2.2
w.-t. FAS	138		

FIGURE 2: Characterization of the two NADPH binding sites of FAS by fluorescence enhancement: G1673Y (open circles), G1888A (closed circles), and wild-type FAS (diamonds). All proteins were C-terminally His-tagged. FAS protein at 3.77 μM was titrated with NADPH. Fluorescence enhancement, fluorescence emittence, and binding parameters were calculated as described in Experimental Procedures. The dashed line represents superimposition of G1888A and G1673Y FAS data.

Incorporation of malonyl moieties into fatty acids by two β-ketoacyl reductase mutants, in the presence of added free CoA, was reduced to less than 1% of that of the wild-type FAS. The only 4-carbon intermediate released from the enzyme in significant quantity was the β-ketobutyryl moiety. This was the expected result, based on the markedly reduced ability of these mutants to bind NADPH required for the β-ketoacyl reductase-catalyzed reaction. Similarly, the ability of the dehydrase mutant (H878A) to convert malonyl-CoA to fatty acid was reduced by more than 2 orders of magnitude, compared to that of the wild-type FAS, and β-hydroxybutyryl moieties, the substrate for the inhibited reaction, leaked off the enzyme by transfer to CoA. The ability of three different enoyl reductase mutants to convert malonyl-CoA to fatty acid was reduced by more than 2 orders of magnitude, compared to that of the wild-type FAS. Surprisingly, in the case of these mutants, not only crotonyl moieties, the substrate for the inhibited enoyl reductase, but also β-hydroxybutyryl and β-ketobutyryl moieties leaked off the enzyme by transfer to CoA. We reasoned that the release of β-hydroxybutyryl moieties from FASs carrying mutations in the enoyl reductase domain could possibly result from an equilibrium in the

Table 3: Products Formed by FASs Carrying Mutations in the β-Carbon Processing Enzymes

		products (nmol of malonyl moieties incorporated/min)[a]					
			CoA esters				fatty
FAS	CoA	TAL	β-keto-C4	β-OH-C4	4:1	4:0	acid
wild type	+	0.44	18.4	1.3	0.47	11.6	155
	0	0.65	6.4	0.68	0.17	3.46	358
G1886F	+	0.66	20.8	0.63	0.30	0	0.61
(KR$^-$)	0	nd	nd	nd	nd	nd	nd
G1888A	+	1.47	20.2	0.63	0.29	0	3.0
(KR$^-$)	0	nd	nd	nd	nd	nd	nd
H878A	+	0.34	1.52	17.5	0	0	0
(DH$^-$)	0	0.15	0.76	2.13	0.04	0	0
G1672V	+	0.06	6.23	2.56	1.65	0	0.12
(ER$^-$)	0	0.84	0.69	0.25	0.16	0	0.94
G1672V/ G1675T	+	0.06	4.0	1.97	1.32	0	0
(ER$^-$)	0	1.1	1.0	0.37	0.20	0	0.26
G1673Y	+	0.07	4.94	1.89	1.48	0	0.29
(ER$^-$)	0	0.72	1.01	0.44	0.24	0	2.1

[a] Product formation was analyzed under steady-state conditions where no more than 10% of the substrate was utilized. Standard deviations for the duplicate assays were less than $\pm$10% in most cases and did not exceed $\pm$20%. Abbreviations: TAL, triacetic lactone; β-keto-C4, β-ketobutyryl; β-OH-C4, β-hydroxybutyryl; 4:1, crotonyl; 4:0, butyryl; KR$^-$, β-ketoacyl reductase knockout; ER$^-$, enoyl reductase knockout. H878A FAS had no tag; wild-type, G1672V, and G1888A FAS were C-terminally His-tagged. All other mutants had a C-terminal FLAG tag.

Table 4: Dehydrase Activity of FAS in the Forward and Backward Directions

direction	substrate	activity (nmol min^{-1} mg^{-1})
forward	*S*-β-hydroxybutyryl-*N*-acetylcysteamine	2.9 ± 0.1[a]
backward	*S*-crotonyl-*N*-acetylcysteamine	27 ± 1.4[a]
forward	β-hydroxybutyryl-CoA	70.1 ± 4.7[b]
backward	crotonyl-CoA	129 ± 0.8[b]

[a] Determined at 300 μM (nonsaturating concentration). [b] V_{max} values.

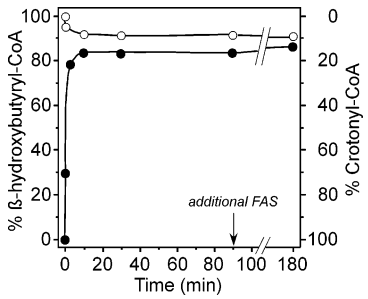

FIGURE 3: Determination of the equilibrium of the dehydrase reaction. The reaction mixtures contained wild-type FAS (170 μg/mL), free CoA (50 μM) as acceptor, and either β-hydroxybutyryl-CoA or crotonyl-CoA (100 μM) as substrate. After 90 min incubation, additional FAS (170 μg/mL) was added to the reaction mixture. The products were identified by HPLC, as described in Experimental Procedures. Key: open circles, forward reaction; closed circles, backward reaction.

dehydrase reaction that favored hydration, rather than dehydration. This possibility was investigated experimentally with the wild-type FAS.

Characterization of the Dehydrase Reaction. The dehydrase reaction traditionally has been monitored in the forward direction, using the *S*-β-hydroxybutyryl thioesters of either *N*-acetylcysteamine or CoA as substrates. The former acts solely as a model substrate and is dehydrated without formation of a covalent acyl-enzyme intermediate, whereas the latter can be transferred, through the action of the broad specificity malonyl/acetyl transferase, to the phosphopantetheinyl moiety of the ACP domain for presentation to the dehydrase and the product transferred back to a CoA acceptor via the same route (*12*). Thus the K_m values for the CoA thioester substrates are determined by the interaction with the malonyl/acetyl transferase domain and are in the micromolar range, whereas the K_m values for the *N*-acetylcysteamine thioester substrates are determined by direct interaction with the dehydrase domain and are in the millimolar range. Since the high absorbance at 270 nm limits the concentration of this substrate that can be used in the spectrophotometric assay, we compared the activities in the forward and backward reaction with *N*-acetylcysteamine thioester substrates at the same, subsaturating concentration. In assays using the CoA thioesters, it was possible to use saturating substrate concentrations. With both types of thioester substrate, activity in the backward direction was higher than in the forward direction (Table 4). The H878A dehydrase mutant was compromised in ability to catalyze both the forward and backward reactions, indicating that the dehydration and hydration reactions are indeed catalyzed by the same domain (data not shown).

The equilibrium of the dehydrase reaction, assessed using the CoA thioester substrates, was found to favor the backward hydration reaction, as suspected (Figure 3). In contrast, neither of the two reductase-catalyzed reactions is reversible to any detectable level (details not shown).

Role of the Central Core Region in Facilitating the β-Carbon Processing Reactions. The region between the dehydrase and enoyl reductase domains, consisting of approximately 600 residues, has not been assigned a catalytic role. Earlier, we identified, in tryptic digests of the FAS, polypeptides originating from this core region that appeared to form dimers spontaneously (*20*), and further support for a role of the central core in stabilization of the dimer subsequently was obtained using the yeast two-hybrid system. Fusion of residues 979−1631 of the human FAS to both the DNA binding and activation domains of GAL4 promoted β-galactosidase expression, as did fusion of residues 979−1295 to the DNA binding domain and fusion of residues 1296−1631 to the activation domain (*21*). These findings suggested that a dimerization domain may be formed through the interaction of the N- and C-terminal halves of the core regions of the two subunits. Similar extensive, noncatalytic core sequence elements are also commonly found in the structurally related modular PKSs which, like the FASs, also function as dimers. Nevertheless, we were intrigued by the observation that a few PKS modules have been characterized that are completely lacking in coding sequences for any of the β-carbon processing enzymes and these modules are completely devoid of core sequence elements; for example, module 2 of the rifamycin PKS (*22*), modules 1 and 2 of the pyoluterin PKS (*23*), and module 12 of the rapamycin PKS (*24*), all of which consist of β-ketoacyl synthase−acyl transferase−ACP domain arrangements, and module 6 of the 10-deoxymethynolide/narbonolide PKS (*25*), which consists of a β-ketoacyl synthase−acyl transferase−ACP−thioesterase ensemble. These modules apparently are

Table 5: Conserved Sequence Element in the Central Core Region of FASs and PKSs

origin	sequence
rat FAS	WGAFRHFQLEQDKP
chicken FAS	WGSFRHLPLQQAQP
human FAS	WGAFRHFLLEEDKP
Caenorhabditis elegans FAS	WGSMRHIVVKDEDV
Drosophila melanogaster FAS	WGSYRHLKMESRPP
Rifamycin PKS module 1	WGLVRSAQSEHPGR
Rifamycin PKS module 3	WGLGRAVALERLDR
Rapamycin PKS modules 9-13	SGLMRSAQSEHPGR
Pyoluteorin PKS module 3	WGLGKTLALEHPEH
Pikromycin PKS module 1	WGLGRVVALEHPER
Pikromycin PKS module 2	WGLVRTAQTENPGR
Pikromycin PKS module 3	WGMGRVAALEHPER
Pikromycin PKS module 4	WGLGRSAQTESPGR
Pikromycin PKS module 5	WGLGRVVALEHPER
Consensus sequence	WG--R----E

perfectly capable of carrying out a chain elongation step, which is believed to require a dimeric module, in the absence of the putative core dimerization domains. We therefore began evaluation of the possibility that the core region was essential for facilitating the β-carbon processing reactions catalyzed by the animal FAS. Initially, we engineered two large deletion constructs Δ1153−1544 and Δ1010−1633. The 1153−1544 deletion was designed to exclude the polypeptide region that we had earlier found to undergo spontaneous dimerization (*20*), and the longer deletion essentially excludes the entire region from the likely C-terminus of the dehydrase into the N-terminal region of the enoyl reductase domain. Both deletion constructs purified predominantly as higher oligomers, although very minimal amounts of dimers were also detected by gel filtration analysis, and both preparations were completely inactive in the overall FAS reaction. Significantly, both deletion constructs were completely lacking in β-ketoacyl reductase and enoyl reductase activities, although catalytic activities of the malonyl/acetyl transacylase and thioesterase domains were preserved. No β-ketoacyl reductase activity was detectable in these FASs even when assayed using *trans*-1-decalone as substrate. This model substrate is reduced by the wild-type FAS without prior formation of a covalent acyl-enzyme intermediate, and activity is observed in both the monomeric and dimeric forms of the FAS.

In an attempt to identify a relatively short sequence element within the core region that might be essential for functioning of the FAS, we performed multiple alignments of sequences from the central core regions of animal FASs and from those modules of the PKSs mentioned above that contain functional β-carbon processing domains. In general, the central core regions are poorly conserved. Nevertheless, we were able to identify a short, relatively well-conserved sequence element within the core region of FASs and modular PKSs (Table 5). This sequence element is present in PKS modules regardless of whether coding regions for dehydrase or enoyl reductase domains are present, so that it is unlikely to play a catalytic role in either of these two domains that flank the central core region. Deletion of this 14-residue sequence from the rat FAS resulted in total loss of FAS activity (Table 6). The "Δ14-FAS" purified as a mixture of mainly higher oligomers with very small amount of dimers and monomers, as monitored by gel filtration analysis. Dynamic light scattering analysis disclosed the presence of only higher oligomeric species, 3.5 ± 0.5 MDa. The higher oligomeric species are built possibly from FAS dimers considering that β-ketoacyl synthase-mediated acyltransferase activity, which requires the dimeric form of the FAS, was ∼61% of that of the wild-type FAS dimer. Nevertheless, the ability of the Δ14-FAS to catalyze the condensation reaction was severely compromised, amounting to only ∼4% of that of the wild-type FAS dimer. The activities of the malonyl/acetyl transacylase and thioesterase domains, assessed using model substrates, were essentially unchanged from those of the wild-type FAS. As in the case of the two large deletion FASs, the Δ14-FAS lacked both reductase activities, and fluorescence enhancement experiments revealed that both types of nucleotide binding sites had been completely eliminated. Dehydrase activity, assayed in the forward direction using the model substrate, was ∼21% of that of the wild-type FAS. Replacement of the 14 residues in the reverse order generated an inactive FAS with properties similar to that of the Δ14-FAS, indicating that disruption of integrity of the protein did not result simply from the introduction of a gap in the sequence (details not shown).

Table 6: Properties of FASs Containing Mutations in the Central Core Region

FAS	sequence (1497-1517)[a]	form[b]	NADPH binding	enzyme activity (% of wild type)[d] FAS	KR	ER	DH	KS-AT	KS-C	MAT	TE
wild type	NVYRDGAWGAFRHFQLEQDKP	dimer	normal	100	100	100	100	100	100	100	100
Δ14	**NAYR**----------**DGP**	oligomer	none	0	0	0	21	61	4	100	93
V/A, K/G[c]	**NAYRDGAWGAFRHFQLEQDGP**	dimer	normal	100	100	nd	100	100	100	112	92
V/A, W/A, K/G	**NAYRDGAAGAFRHFQLEQDGP**	oligomer	none	0	0	0	nd	19	0	52	43
R1508K	NVYRDGAWGAF**K**HFQLEQDKP	dimer + oligomer	nd	58	68	nd	nd	nd	nd	77	74
R1508D	NVYRDGAWGAF**D**HFQLEQDKP	dimer + oligomer	nd	14	14	nd	nd	nd	nd	68	59
R1508A	NVYRDGAWGAF**A**HFQLEQDKP{	purified oligomer purified dimer	none normal	0 100	0 80	0 97	19 93	53 100	3 79	64 86	53 95

[a] Mutated residues are highlighted in boldface characters. [b] FAS preparations were characterized by gel filtration and dynamic light scattering. The Δ14 and V/A, W/A, K/G FAS preparations consisted entirely of the higher oligomeric form (>2 MDa), the R1508D and R1508A mutant FAS preparations consisted predominantly of higher oligomers (>70%), and the R1508K mutant was mostly in the dimeric form (≥80%). [c] The V1498A and K1516G mutations initially were introduced to engineer restriction sites in the cDNA that facilitated replacement mutagenesis but were restored in the R1508 mutants. [d] Specific activities determined for the wild-type FAS were 1930 ± 40, 20220 ± 250, 1340 ± 25, 131 ± 1, 154 ± 1, 74 ± 1, 2520 ± 170, and 1120 ± 20 nmol min^{-1} mg^{-1} for FAS, KR, ER, DH, KS-AT, KS-C, MAT, and TE assays, respectively. All determinations were done at least twice. Standard deviations were lower than 7% of the value shown in the table. KS-AT and KS-C are decanoyl transferase and β-ketobutyryl-CoA synthase activity of the β-ketoacyl synthase domain, respectively. nd = not determined.

Single-residue mutagenesis within this region revealed that mutations at either W1504 (in the context of the benign V1498A, K1516G double mutation) or R1508 alone was sufficient to eliminate the two types of nucleotide binding sites and cause the formation of higher oligomers. The effect of introduction of mutations at R1508 was studied in detail. The R1508K mutant had properties similar to that of the wild type, whereas the R1508D/A mutants purified mainly as higher oligomers with impaired properties. Approximately 80% of the R1508A FAS expressed in *Sf*9 cells could be purified as the high molecular mass oligomeric form estimated by gel filtration to be above 2 MDa (void volume) and by dynamic light scattering to be 16.6 ± 0.2 MDa. Higher oligomeric forms were inactive in the overall FAS reaction and unable to bind NADPH. However, ~20% of the expressed R1508A FAS was purified in the dimeric form and exhibited normal NADPH binding and normal FAS activity. This R1508A dimer could be reversibly dissociated into monomers under the same conditions used to interconvert wild-type dimers and monomers. However, the higher oligomeric form of R1508A could not be dissociated into monomers under the same conditions.

DISCUSSION

The location of the nucleotide binding regions in the β-ketoacyl reductase and enoyl reductase domains of the FAS has been ascertained unequivocally, and the importance of the presence of the conserved glycine residues in the predicted Rossmann fold has been verified by mutagenesis. Earlier attempts to characterize the pyridine nucleotide binding sites of avian and mammalian FASs that employed either fluorescence enhancement or equilibrium dialysis were hampered by an inability to distinguish clearly between the β-ketoacyl reductase and enoyl reductase binding sites and relied on the assumption that the fluorescence enhancement associated with NADPH binding was the same for all sites (*26*−*29*). These studies concluded that the FAS contained two to four binding sites per dimer and disagreed as to whether the binding sites were identical. However, Poulose et al. (*30*) devised a new analytical procedure that did not assume similar enhancement factors and estimated that the FAS contained two pairs of binding sites per dimer with different affinities and different enhancement factors. By using pyridoxal phosphate to inactivate specifically the binding site in the enoyl reductase domain, the authors deduced that the site with low affinity (K_d 7 μM) and higher enhancement (800 F μM^{-1}) was associated with the β-ketoacyl reductase domain and that with higher affinity (K_d 1.3 μM) and lower enhancement (400 F μM^{-1}) was associated with the enoyl reductase domain. The engineering of mutant FASs defective in only one of the two nucleotide binding sites in the present study has permitted unambiguous characterization of the two sites individually. Both kinetic experiments and direct measurement of the fluorescence enhancement accompanying nucleotide binding confirmed the earlier findings of Poulose et al. that the binding site in the enoyl reductase domain exhibits higher fluorescent enhancement and lower binding affinity than that associated with the β-ketoacyl reductase domain. NADH is a relatively ineffective hydrogen donor for both reductases.

In addition to synthesizing long-chain fatty acid, the wild-type FAS releases small amounts of the 4-carbon intermediates, β-ketobutyryl, β-hydroxybutyryl, crotonyl, and butyryl moieties, by transfer to CoA. Whereas FASs compromised by mutations in any of the β-carbon processing domains have little or no ability to synthesize long-chain fatty acids, they retain the ability to dispose of the 4-carbon intermediates that are stalled on the protein, by transfer to CoA. In the case of the β-ketoacyl reductase and dehydrase mutants, the major 4-carbon moieties released are those that are the substrates for the mutated domain, that is, the β-ketobutyryl and β-hydroxybutyryl moieties, respectively. Surprisingly, we found that the enoyl reductase-defective FAS mutant releases not only crotonyl moieties but also the upstream intermediates, β-hydroxybutyryl and β-ketobutyryl moieties. Although the two reductase reactions are essentially irreversible, the dehydrase catalyzes the reverse hydration reaction more efficiently than the forward dehydration reaction. Furthermore, the equilibrium in this reaction lies toward substrate rather than product formation. These findings explain, at least in part, the observation that several downstream intermediates are shed from the FAS enoyl reductase mutant and reveal an unanticipated similarity between the type I FAS and its type II counterpart in *Escherichia coli* (*31*) in that, in both systems, the equilibrium in the dehydration reaction favors formation of the β-hydroxy over the enoyl intermediate by a ratio of approximately 9:1. Thus, in both systems the enoyl reductase plays a critical role in pulling the β-carbon processing reactions toward product formation.

In a seminal investigation, an enoyl reductase knockout mutation was previously introduced to module 4 of the polyketide synthase responsible for the production of erythromycin by *Saccharopolyspora erythraea* (*32*). In this case two adjacent glycine residues within the putative NADPH binding region of the enoyl reductase (positionally equivalent to Gly 1672 and Gly 1673 in the rat FAS) were replaced with Ser-Pro. The major product formed by the modified polyketide synthase was identified as $\Delta^{6,7}$-anhydroerythromycin C, as expected if the enoyl intermediate produced by module 4 is elongated by the β-ketoacyl synthase of module 5. In retrospect, it is intriguing that the β-hydroxy equilibrium intermediate formed by module 4 was not elongated. Two possible explanations come to mind. It is possible that the dehydrases associated with polyketide synthases differ from those involved in fatty acid synthesis in that the equilibrium favors the forward (dehydration) reaction. Alternatively, the β-hydroxy intermediate may be a very poor substrate for the β-ketoacyl synthase of module 5. The first possibility seems rather unlikely, in view of the overall structural similarity of the intermediates of the two pathways and the general rule that enzymes do not change the equilibria of catalyzed reactions. The mutant strain produces $\Delta^{6,7}$-anhydroerythromycin C at only one-fifth of the rate that the wild-type strain produces erythromycin A, suggesting that perhaps the enoyl intermediate is not as good a substrate as is the saturated intermediate for the β-ketoacyl synthase of module 5. Thus it is possible that β-ketoacyl synthases can act as "gatekeepers" by discriminating against certain of the intermediates produced by the upstream module. In this particular case, the β-hydroxy intermediate produced by the mutated module 4 may be a very poor substrate for the β-ketoacyl synthase of module 5. This possible explanation conceivably could be tested experimentally by replacing, in the context of the

module 4 enoyl reductase mutant, the β-ketoacyl synthase of module 5 with a β-ketoacyl synthase that is known to accept β-hydroxy intermediates as substrates for elongation.

Our supposition that the absence of central core regions in those PKS modules that lack β-ketoacyl reductase, dehydrase, and enoyl reductase domains might indicate a role for these sequence elements in facilitating β-carbon processing reactions in PKSs and FASs appears meritorious, since deletions and replacements in this region could be identified that completely eliminate reductase activity in FAS. The loss in β-ketoacyl reductase and enoyl reductase activities observed with the Δ1153−1544, Δ1010−1633, and Δ1501−1514 core deletions and the W1504A mutation could be accounted for entirely by the elimination of NADPH binding in the two reductase domains. All of these core mutations also caused the FAS to form higher oligomers containing at least eight subunits. However, the aberrant oligomerization apparently cannot be attributed to global misfolding of the FAS polypeptide chain, since activities of the acyl transferase of β-ketoacyl synthase, malonyl/acetyl transacylase, and thioesterase domains, located near the N-terminus and the C-terminus, typically are retained in these mutants. Similarly, dehydrase domain activity is retained, albeit reduced by 75−80%. Unlike KS acyl transferase activity, KS condensation activity is practically abolished, indicating lack of communication in the pathway providing substrates for the condensation. We suspect, therefore, that mutations in the central core may result in improper folding of the core region that compromises the ability of the protein to undergo normal dimerization, resulting in the formation of higher oligomers that retain some partial activities but are unable to bind NADPH and to provide substrates for the condensation reaction. The R1508A single mutant is particularly intriguing, since this FAS can form two species, with quite different conformations, that can be readily separated from each other and are not interconvertible. One species is dimeric and has nucleotide binding and catalytic properties essentially indistinguishable from those of the wild-type FAS. In addition, this species can be reversibly dissociated into monomers under the same conditions that effect interconversion of wild-type FAS dimers and monomers. The only significant difference from the wild-type FAS dimers that we have noticed is that the R1508A dimers are markedly less heat stable than are those of the wild type (details not shown). The R1508 higher oligomeric species exhibits properties similar to those described above for the core deletion mutants; i.e., they are unable to bind NADPH and catalyze the condensation reaction and therefore are inactive in the overall FAS reaction. Unlike the dimeric form of the R1508A FAS, the higher oligomeric form cannot readily be dissociated into monomers. This higher oligomeric form of the R1508A FAS, in common with the Δ1501−1514 and the W1504A FASs, retains in part the ability to catalyze the β-ketoacyl synthase-mediated acyl-transfer reaction, which was earlier shown to be catalyzed by the dimeric, but not the monomeric, form of the wild-type FAS (*33*). Thus some features characteristic of normally juxtaposed subunit pairs may be preserved within the context of the higher oligomers. A plausible explanation for these findings is that the R1508A mutant represents a marginal case in which, at a critical stage in folding of the core region, either a normal or aberrant pathway can be followed. If normal folding occurs, then oligomerization is limited to formation of the dimer, which exhibits near-normal properties, but misfolding at this stage results in the irreversible formation of higher oligomers, which are unable to bind NADPH, catalyze the condensation reaction, or efficiently catalyze the dehydrase reaction.

A role for the central core in the dimerization process had been suggested earlier, and this study reveals that certain deletions and mutations in the central core region can lead to the adoption of conformations that do not allow proper dimerization of the FAS. More surprising, perhaps, is the finding that deletions, and even single-site mutations, in the core region can disrupt entirely the NADPH binding sites located distantly toward the C-terminus of the FAS. As indicated above, the structurally similar modular PKSs, which also function as dimeric units, lack comparable central core sequences only in those modules that are completely devoid of β-carbon processing domains. We suggest, therefore, that the central core region may be required for the adoption of a specific conformation that facilitates nucleotide binding and access of intermediates to the β-carbon processing enzymes in the FASs and modular PKSs.

NOTE ADDED IN PROOF

A genome-wide linkage scan for genetic determinants of obesity in Pima Indians has identified a Val1483Ile polymorphism in the FAS gene of full-blooded, nondiabetic individuals that is associated with lower body fat content (*34*). The authors suggest that the mutation may result in lowered cellular FAS activity that could be protective against obesity. The valine residue in question is positionally conserved in all vertebrate FASs (residue 1476 in rat) and is located in the central core near the site targeted for mutagenesis in our study.

ACKNOWLEDGMENT

We thank Dr. Robert Ryan for use of his luminescence spectrometer and Drs. Gerry McDermott and Christine Trame of the Lawrence Berkeley National Laboratory for making their DynaPro-MS/X available to us and for their valuable help with experiments.

SUPPORTING INFORMATION AVAILABLE

Details of the procedures used to construct replacement and deletion mutations in the core region of the FAS. This material is available free of charge via the Internet at http://pubs.acs.org.

REFERENCES

1. Wakil, S. J. (1989) Fatty acid synthase, a proficient multifunctional enzyme, *Biochemistry 28*, 4523−4530.
2. Smith, S., Witkowski, A., and Joshi, A. K. (2003) Structural and functional organization of the animal fatty acid synthase, *Prog. Lipid Res. 42*, 289−317.
3. Chang, S. I., and Hammes, G. G. (1990) Structure and mechanism of action of a multifunctional enzyme complex: fatty acid synthase, *Acc. Chem. Res. 23*, 363−369.
4. Joshi, A. K., and Smith, S. (1993) Construction, expression and characterization of a mutated animal fatty acid synthase deficient in the dehydrase function, *J. Biol. Chem. 268*, 22508−22513.
5. Rost, B. (1996) PHD: predicting 1D protein structure by profile based neural networks, *Methods Enzymol. 266*, 525−539.
6. Amy, C., Witkowski, A., Naggert, J., Williams, B., Randhawa, Z., and Smith, S. (1989) Molecular cloning and sequencing of

cDNAs encoding the entire rat fatty acid synthetase, *Proc. Natl. Acad. Sci. U.S.A. 86*, 3114−3118.
7. Rangan, V. S., Joshi, A. K., and Smith, S. (2001) Mapping the functional topology of the animal fatty acid synthase by mutant complementation in vitro, *Biochemistry 40*, 10792−10799.
8. Rossmann, M. G., Liljas, A., Bränden, C. I., and Banaszak, L. J. (1975) Evolutionary and structural relationships among dehydrogenases, in *The Enzymes* (Boyer, P. D., Ed.) pp 61−102, Academic Press, New York.
9. Scrutton, N. S., Berry, A., and Perham, R. N. (1990) Redesign of the coenzyme specificity of a dehydrogenase by protein engineering, *Nature 343*, 38−43.
10. Joshi, A. K., and Smith, S. (1993) Construction of a cDNA encoding the multifunctional animal fatty acid synthase and expression in *Spodoptera frugiperda* cells using baculoviral vectors, *Biochem. J. 296*, 143−149.
11. Witkowski, A., Joshi, A. K., and Smith, S. (1996) Fatty acid synthase: *In vitro* complementation of inactive mutants, *Biochemistry 35*, 10569−10575.
12. Joshi, A. K., Witkowski, A., and Smith, S. (1997) Mapping of functional interactions between domains of the animal fatty acid synthase by mutant complementation in vitro, *Biochemistry 36*, 2316−2322.
13. Witkowski, A., Joshi, A. K., Rangan, V. S., Falick, A. M., Witkowska, H. E., and Smith, S. (1999) Dibromopropanone cross-linking of the phosphopantetheine and active-site cysteine thiols of the animal fatty acid synthase can occur both inter- and intra-subunit: Re-evaluation of the side-by-side, antiparallel subunit model, *J. Biol. Chem. 274*, 11557−11563.
14. Shyamala, V., and Ames, G. F.-L. (1991) Use of exonuclease for rapid polymerase-chain-reaction-based in vitro mutagenesis, *Gene 97*, 1−6.
15. Joshi, A. K., Rangan, V. S., and Smith, S. (1998) Differential affinity-labeling of the two subunits of the homodimeric animal fatty acid synthase allows isolation of heterodimers consisting of subunits that have been independently modified, *J. Biol. Chem. 273*, 4937−4943.
16. Pry, T. A., and Hsu, R. Y. (1980) Equilibrium substrate binding studies of the malic enzyme of pigeon liver. Equivalence of nucleotide sites and anticooperativity associated with the binding of L-malate to the enzyme-manganese (II)-reduced nicotinamide adenine dinucleotide phosphate ternary complex, *Biochemistry 19*, 951−962.
17. Naggert, J., Narasimhan, M. L., De Veaux, L., Cho, H., Randhawa, Z. I., Cronan, J. E., Jr., Green, B. N., and Smith, S. (1991) Cloning, sequencing, and characterization of *Escherichia coli* thioesterase II, *J. Biol. Chem. 266*, 11044−11050.
18. Kitamoto, T., Nishigai, M., Sasaki, T., and Ikai, A. (1988) Structure of fatty acid synthase from the harderian gland of guinea pig, *J. Mol. Biol. 203*, 183−195.
19. Stoops, J. K., Wakil, S. J., Uberbacher, E. C., and Bunick, G. J. (1987) Small-angle neutron-scattering and electron microscope studies of the chicken liver fatty acid synthase, *J. Biol. Chem. 262*, 10246−10251.
20. Witkowski, A., Rangan, V. S., Randhawa, Z. I., Amy, C. M., and Smith, S. (1991) Structural organization of the multifunctional animal fatty-acid synthase, *Eur. J. Biochem. 198*, 571−579.
21. Chirala, S. S., Jayakumar, A., Gu, Z. W., and Wakil, S. J. (2001) Human fatty acid synthase: Role of interdomain in the formation of catalytically active synthase dimer, *Proc. Natl. Acad. Sci. U.S.A. 98*, 3104−3108.
22. August, P. R., Tang, L., Yoon, Y. J., Ning, S., Muller, R., Yu, T. W., Taylor, M., Hoffmann, D., Kim, C. G., Zhang, X., Hutchinson, C. R., and Floss, H. G. (1998) Biosynthesis of the ansamycin antibiotic rifamycin: deductions from the molecular analysis of the rif biosynthetic gene cluster of *Amycolatopsis mediterranei S699*, *Chem. Biol. 5*, 69−79.
23. Nowak-Thompson, B., Gould, S. J., and Loper, J. E. (1997) Identification and sequence analysis of the genes encoding a polyketide synthase required for pyoluteorin biosynthesis in *Pseudomonas fluorescens Pf-5*, *Gene 204*, 17−24.
24. Schwecke, T., Aparicio, J. F., Molnar, I., König, A., Khaw, L. E., Haydock, S. F., Oliynyk, M., Caffrey, P., Cortes, J., Lester, J. B., Böhm, G. A., Staunton, J., and Leadlay, P. F. (1995) The biosynthetic gene cluster for the polyketide immunosuppressant rapamycin, *Proc. Natl. Acad. Sci. U.S.A. 92*, 7839−7843.
25. Beck, B. J., Yoon, Y. J., Reynolds, K. A., and Sherman, D. H. (2002) The hidden steps of domain skipping: macrolactone ring size determination in the pikromycin modular polyketide synthase, *Chem. Biol. 9*, 575−583.
26. Dugan, R. E., and Porter, J. W. (1970) The binding of reduced nicotinamide adenine dinucleotide phosphate to mammalian and avian fatty acid synthetases—number of binding sites and the effect of reagents and conditions on the binding of reduced nicotinamide adenine dinucleotide phos, *J. Biol. Chem. 245*, 2051−2059.
27. Hsu, R. Y., and Wagner, B. J. (1970) Reduced triphosphopyridine nucleotide binding sites of the fatty acid synthetase of chicken liver, *Biochemistry 9*, 245−251.
28. Srinivasan, K. R., and Kumar, S. (1976) Reduced nicotinamide adenine dinucleotide phosphate, a structural and conformational probe of chicken liver fatty acid synthetase, *J. Biol. Chem. 251*, 5352−5360.
29. Cardon, J. W., and Hammes, G. G. (1982) Investigation of reduced nicotinamide adenine dinucleotide phosphate and acyl-binding sites on avian fatty acid synthase, *Biochemistry 21*, 2863−2870.
30. Poulose, A. J., Foster, R. J., and Kolattukudy, P. E. (1980) New fluorescence evidence that each peptide of fatty acid synthetase has a keto and an enoyl reductase domain with different affinities for NADPH, *J. Biol. Chem. 255*, 11313−11319.
31. Heath, R. J., and Rock, C. O. (1995) Enoyl-acyl carrier protein reductase (*fabI*) plays a determinant role in completing cycles of fatty acid elongation in *Escherichia coli*, *J. Biol. Chem. 270*, 26538−26542.
32. Donadio, S., McAlpine, J. B., Sheldon, P. J., Jackson, M., and Katz, L. (1993) An erythromycin analogue produced by reprogramming polyketide synthesis, *Proc. Natl. Acad. Sci. U.S.A. 90*, 7119−7123.
33. Witkowski, A., Joshi, A. K., and Smith, S. (2002) Mechanism of the β-ketoacyl synthase reaction catalyzed by the animal fatty acid synthase, *Biochemistry 41*, 10877−10887.
34. Kovacs, P., Harper, I., Hanson, R. L., Infante, A. M., Bogardus, C., Tataranni, P A., and Baier, L. J. (2004) *Diabetes 53*, 1915−1919.

BI048988N